



Universiteit  
Leiden

The Netherlands

## Evolutionary adaptability of $\beta$ -lactamase: a study of inhibitor susceptibility in various model systems

Alen, I. van

### Citation

Alen, I. van. (2023, September 20). *Evolutionary adaptability of  $\beta$ -lactamase: a study of inhibitor susceptibility in various model systems*. Retrieved from <https://hdl.handle.net/1887/3641470>

Version: Publisher's Version

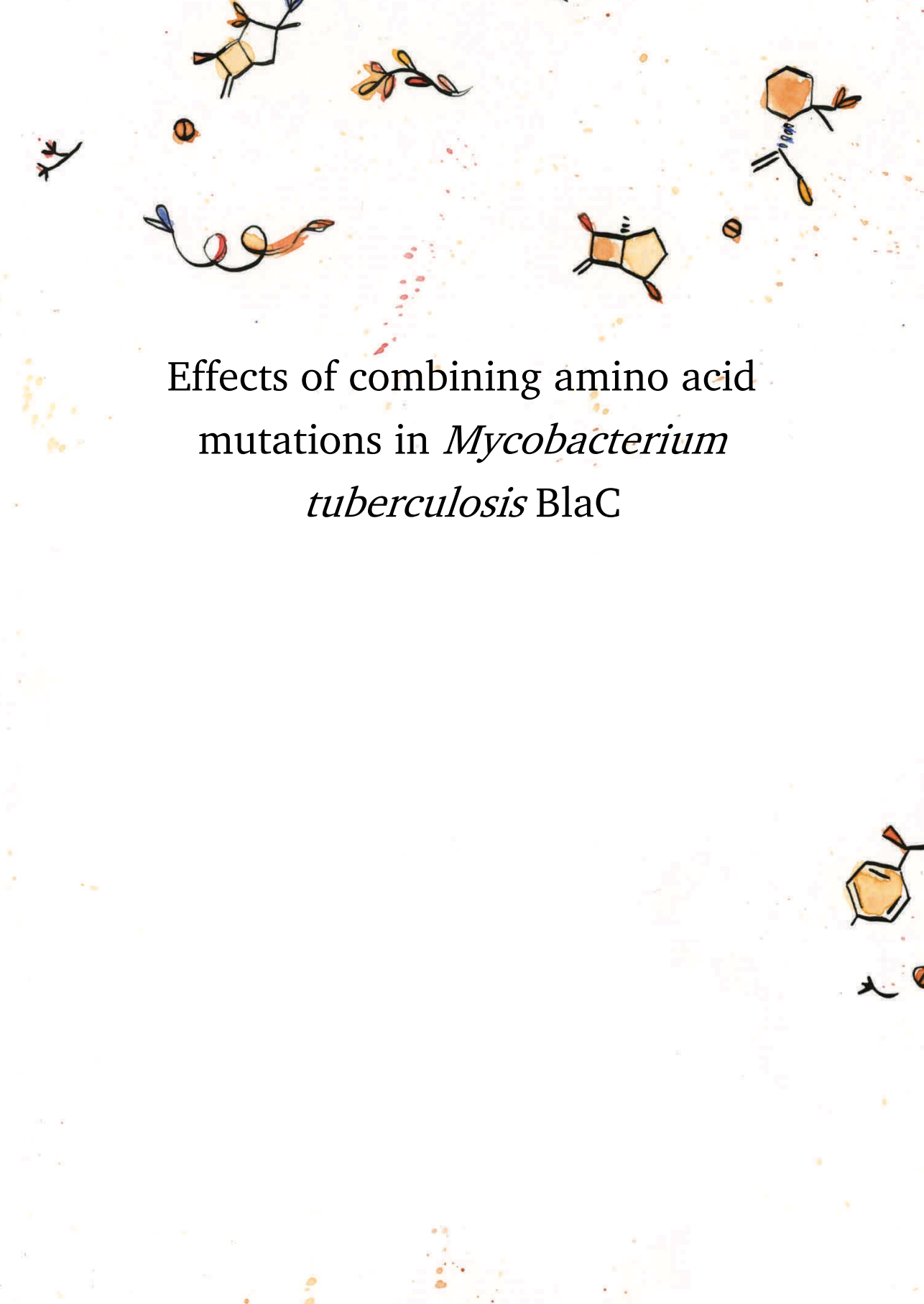
License: [Licence agreement concerning inclusion of doctoral thesis in the Institutional Repository of the University of Leiden](#)

Downloaded from: <https://hdl.handle.net/1887/3641470>

**Note:** To cite this publication please use the final published version (if applicable).

4





Effects of combining amino acid mutations in *Mycobacterium tuberculosis* BlaC

## Abstract

Epistasis is an important phenomenon in protein evolution that complicates the prediction of evolutionary pathways. Three previously characterized mutations, I105F, G132S, and D179N, each have a different effect on the  $\beta$ -lactamase from *Mycobacterium tuberculosis*, BlaC. Here, we studied the effects of combining these mutations. Mutation I105F results in faster hydrolysis of ampicillin, while *Escherichia coli* cells producing BlaC D179N can grow on higher concentrations of ampicillin and avibactam and the protein is more stable. The results show that combining I105F and D179N leads to a positive epistatic effect for ampicillin and results in a more thermostable enzyme, with a melting temperature of 3 °C higher than that of the wild-type enzyme. Adding either I105F or D179N to BlaC G132S allows cells producing these variants to grow on higher concentrations of sulbactam, but mutations I105F and D179N are not able to compensate for the sensitivity of BlaC G132S to avibactam. We discuss that an increase in stability of BlaC can decrease the sensitivity of cells to sulbactam, but not to avibactam. Sulbactam is a slowly converted substrate and an increase in active protein will result in faster conversion, while avibactam acts as a stable reversible inhibitor. In BlaC G132S, the loop covering the active site resembles that of other class A  $\beta$ -lactamases that are sensitive to avibactam indicating that structural changes are likely to be the cause of the increase in sensitivity.

## Introduction

Epistasis is the phenomenon that the effect of a mutation on a protein is dependent on genetic background, and the effect of two mutations is not equal to the sum of the individual effects. Epistasis is important in protein evolution, as it affects the order in which mutations can be acquired and the evolutionary paths a protein can take.<sup>21,22</sup> It also complicates the prediction of mutational effects on proteins.

The  $\beta$ -lactamase from *Mycobacterium tuberculosis*, BlaC, is an extended spectrum  $\beta$ -lactamase that can hydrolyze a broad spectrum of  $\beta$ -lactam antibiotics. While the wild-type enzyme can be inhibited with inhibitors, several point mutations have been found to reduce the sensitivity for them. Residue Ile105 (Ambler numbering<sup>65</sup>) is present in a loop that covers the active site of BlaC (Figure 4.1). Most other class A  $\beta$ -lactamases, like CTX-M-14 and TEM-1, have a tyrosine (64%), histidine, or asparagine (both 11%) in this position, while isoleucine is only present in 3%.<sup>127</sup> The mutation of this residue to Phe was discovered during directed evolution experiments selecting for higher resistance of *Escherichia coli* host cells against ampicillin.<sup>125</sup> The increase in activity is caused by a 3-fold increase in catalytic activity compared to the wild-type enzyme and an increase in the expression level of the mutant gene. This increase in activity was also observed in the presence of the inhibitor clavulanic acid. Modeling of a Phe in position 105 mirroring the position of Tyr in TEM-1 shows a widening of the active site by 3.6 Å compared to wild-type BlaC.<sup>125</sup> It was hypothesized that Ile105 functions as a “gatekeeper” residue and is involved in substrate binding.<sup>125,185,186</sup>

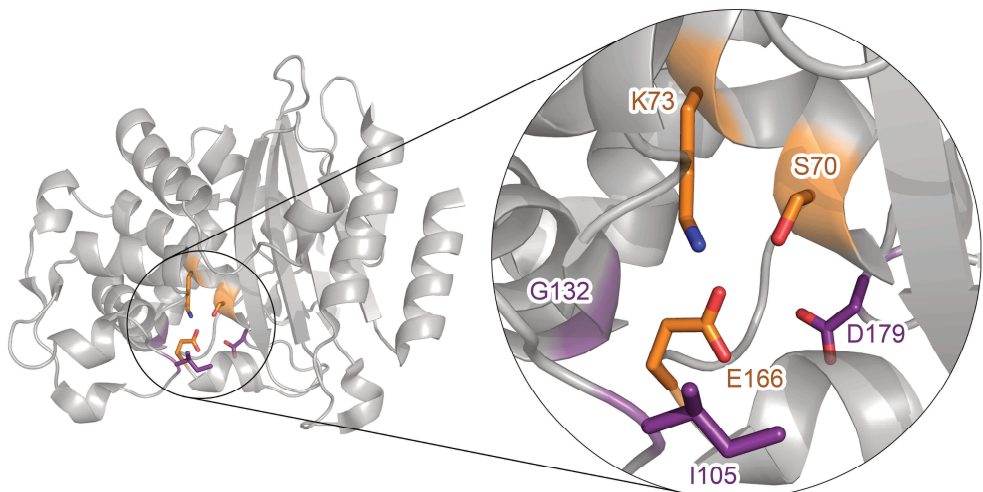


**Figure 4.1.** Position of residues Ile105, Gly132, and Asp179 in BlaC. Crystal structures of BlaC (PDB entry 2GDN<sup>53</sup>), with the side chains of the active site residues Ser70, Lys73, and Glu166 represented as orange sticks. The residues discussed in this chapter, Ile105, Gly132, and Asp179 are shown in purple.

Another mutation found in directed evolution experiments is G132S (chapter 2).<sup>172</sup> Class A  $\beta$ -lactamases have a conserved SDN motif formed by residues 130-132, positioned in the active site. However, in BlaC, position 132 is occupied by a Gly, and restoring the canonical motif has been shown to increase resistance against clavulanic acid.<sup>116</sup> Mutation G132S confers more resistance against the inhibitor sulbactam both *in vivo* and *in vitro*. The  $K_i$  value for sulbactam is 5-fold higher for BlaC G132S than for wild-type BlaC. Interestingly, the catalytic activity of this BlaC variant is 5-fold lower for nitrocefin and 2-fold lower for ampicillin than for the wild type. The crystal structure of BlaC G132S shows that the side chain of Ser132 affects the gatekeeper loop and residue Ile105. The peptide bond between residues Ser104 and Ile105 changes from *trans* to *cis* conformation, the side chain of Ser104 flips away from the active site, and the side chain of Ile105 shifts 1.6 Å towards the entrance of the active site (chapter 2).<sup>172</sup>

Residue Asp179 is positioned in the  $\Omega$ -loop and 99.8% conserved among Class A  $\beta$ -lactamase, yet mutating this residue to asparagine in BlaC leads to a more stable enzyme, while the catalytic activity is similar (chapter 3).<sup>127</sup> *In vivo* data showed that this variant enables *E. coli* to grow on higher concentrations of ceftazidime and avibactam than wild-type BlaC can. This increase in activity against ceftazidime was also observed for the analogous mutants of the  $\beta$ -lactamases KPC-2 and NMC-A. However, cells producing the D179N variants of these  $\beta$ -lactamases grew less in the presence of other substrates and showed lower expression levels (chapter 3).<sup>161</sup> Lower expression levels and lower activity for a broad range of substrates were also found for the D179N variants of TEM-1 and CTX-M-14. The crystal structure of BlaC D179N shows two flipped peptide bonds: between residues 174 and 175 and between 178 and 179, and the latter results in the loss of two salt bridges and increased flexibility of the  $\Omega$ -loop (chapter 3).

Here, we studied the effect of combining three mutations in BlaC, I105F, G132S, and D179N, to elucidate possible epistatic interactions. Given the phenotypes of these BlaC variants and their advantages relative to the wild-type enzyme, it was explored whether these different effects could be combined in one BlaC variant and whether *in vivo* resistance against one inhibitor is compatible with resistance against another. It was found that combining two mutations can result in positive epistasis, increasing the *in vivo* resistance of BlaC against sulbactam in the case of I105F+G132S and I105F+D179N, and allowing *E. coli* cells producing BlaC I105F+D179N to grow on higher concentrations of ampicillin than cells producing the BlaC variants with the single mutations. The sensitivity of BlaC G132S to avibactam could not be compensated by the other two mutations. In conclusion, additive, positive epistatic, and negative epistatic effects were observed when combining mutations I105F, G132S, and D179N in BlaC.

## Results

To assess the *in vivo* activity, the *blaC* genes coding for the single, double, or triple mutants were expressed in liquid *E. coli* cultures and applied to plates containing the antibiotic ampicillin (Figure 4.2, S4.1). The cultures expressing the single mutants of BlaC grew as expected. Cells producing BlaC I105F grew on plates with 100  $\mu\text{g mL}^{-1}$  ampicillin, while those producing wild-type BlaC only grow up to 40  $\mu\text{g mL}^{-1}$  ampicillin. Mutation G132S does not and D179N only slightly increases the *in vivo* activity against ampicillin, as also reported in chapters 2 and 3. Combining two of the three mutations results in different phenotypes. Unsurprisingly, cells expressing BlaC G132S+D179N have similar activity on ampicillin as ones expressing wild type. BlaC I105F+G132S shows slightly lower *in vivo* activity than BlaC I105F, but cells are still able to grow on 100  $\mu\text{g mL}^{-1}$  ampicillin. However, the effect of cells producing BlaC I105F+D179N is slightly bigger than the sum of effects observed for cells with either of the single mutants, showing positive epistasis. The triple mutant has the same phenotype as BlaC I105F+G132S, indicating that the presence of mutation G132S abolishes the synergistic effect of combining I105F and D179N, so a form of negative epistasis (Figure 4.3).

Next, the ability to enhance resistance against the inhibitors sulbactam and avibactam in the presence of ampicillin was tested. BlaC G132S shows enhanced resistance against sulbactam (chapter 2) and cells producing BlaC I105F can grow on 2  $\mu\text{g mL}^{-1}$  sulbactam, whereas cells expressing wild-type BlaC or BlaC D179N cannot (Figures 4.2, S4.2). This enhanced resistance of BlaC I105F can be explained by the increased catalytic activity for ampicillin and adding the mutation D179N to BlaC I105F does not alter this effect. However, combining either or both mutations with G132S resulted in a small synergistic effect as it increased the resistance against sulbactam more than the sum of the single mutants. Cells producing BlaC I105F or BlaC D179N grow better or marginally better than cells producing wild-type BlaC on avibactam, respectively, and the ones harboring BlaC G132S are more sensitive (chapters 2 and 3). Interestingly, BlaC G132S+I105F and BlaC G132S+D179N show negative epistasis for avibactam, as the effect of the double mutations is equal to the effect of BlaC G132S alone, and the same is the case for the triple mutant (Figures 4.2, 4.3, and S4.3). BlaC I105F+D179N shows the same effect as BlaC I105F and should be tested on higher concentrations of avibactam to determine possible epistatic effects (Figure S4.3).

To evaluate if the differences in activity could be caused by changes in the amount of active protein as a result of protein stability, the melting temperature of each of the BlaC variants was determined. BlaC I105F and BlaC D179N show an increase in melting temperature of  $1.5 \pm 0.7$  °C and  $1.9 \pm 0.7$  °C, respectively, compared to wild type (Table 4.1, Figure 4.3). Combining these two mutations results in a melting temperature of  $55.4 \pm 0.5$  °C,  $3.2 \pm 0.7$  °C higher than for wild-type BlaC and indicating that the effects are additive. Mutation G132S causes a small decrease in melting temperature here, although we previously reported no effects

(chapter 2). The addition of G132S to BlaC I105F or BlaC D179N does not significantly change the thermostability.

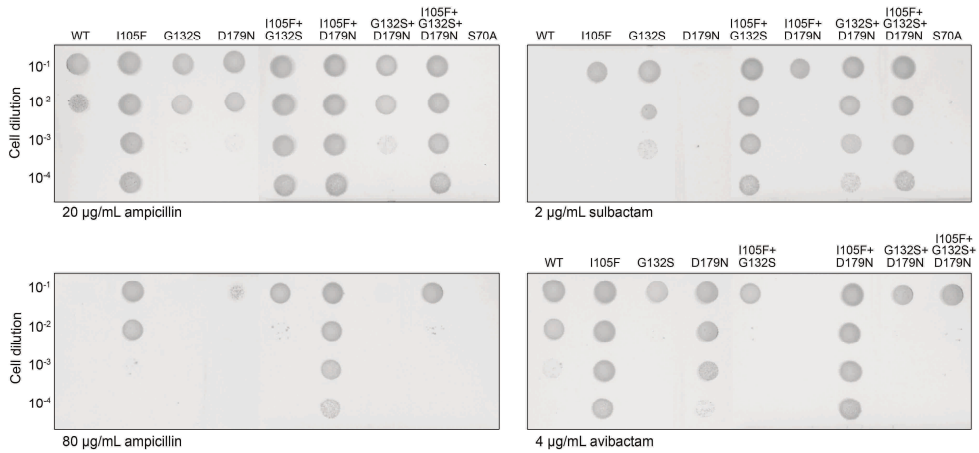


**Figure 4.2.** *In vivo* activity of BlaC variants in *E. coli*. Cells producing the different BlaC variants were spotted in increasing dilution on plates that contained either only ampicillin or the inhibitor sulbactam or avibactam in the presence of 10 µg mL<sup>-1</sup> ampicillin. BlaC S70A is catalytically inactive and functions as negative control. The whole plates are shown in Figure S4.1-S4.3.

**Table 4.1.** Thermostability of BlaC variants. The melting temperatures of single, double, and triple mutants were determined using the dye SYPRO Orange. The measurements were performed in triplicate.

BlaC variant	T <sub>m</sub> <sup>a</sup> (°C)	Δ T <sub>m</sub> <sup>b</sup> (°C)
WT	52.2	
I105F	53.8	1.5
G132S	51.3	-0.9
D179N	54.1	1.9
I105F+G132S	53.3	1.1
I105F+D179N	55.4	3.2
G132S+D179N	53.9	1.7
I105F+G132S+D179N	55.4	3.2

<sup>a</sup> Error 0.5 °C. <sup>b</sup> Propagated error 0.7 °C.



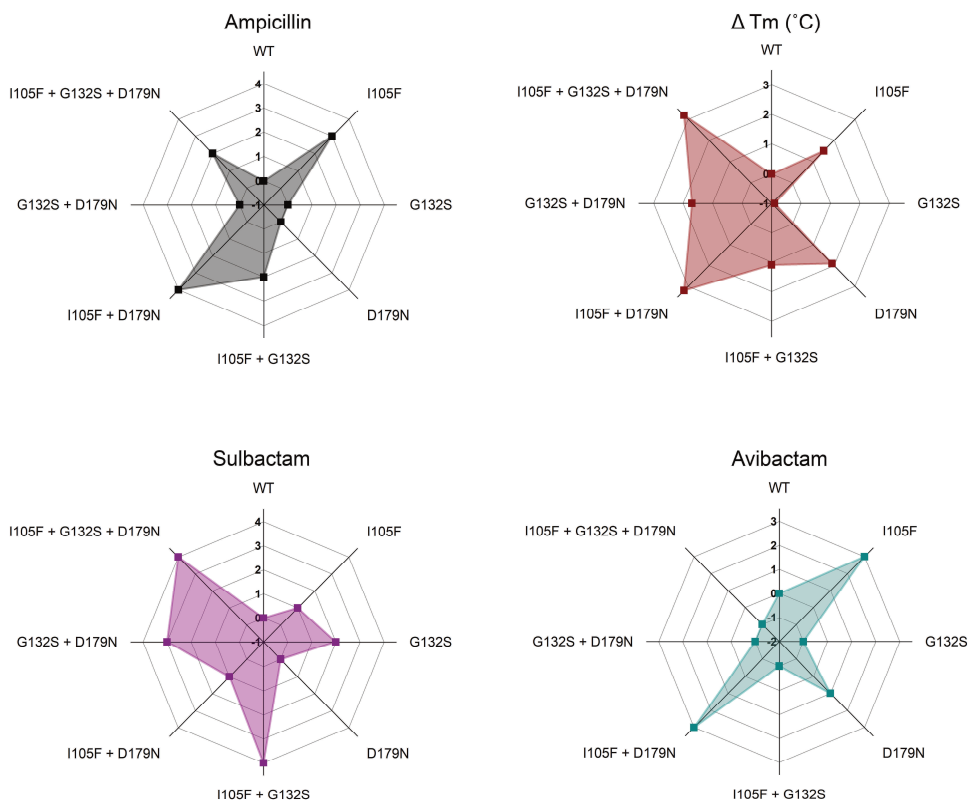


**Figure 4.3.** Graphical representation of differences in activity *in vivo* and thermostability for BlaC variants. The average change in resistance of the BlaC variants compared to wild-type BlaC based on the growth on plates containing ampicillin, sulbactam, or avibactam is represented as squares (e.g. when the maximal dilution of growing cells for wild type is  $10^{-1}$  and for the mutant  $10^{-4}$ , this mutant is scored “3”).

### NMR spectra show the additive effect of mutations on chemical shift perturbations

To analyze the effect of the mutations on the chemical environment of the backbone amides, TROSY-HSQC spectra were measured for purified  $^{15}\text{N}$ -labeled BlaC variants. Peaks were assigned by comparing them to peaks in TROSY-HSQC and HNCA spectra of wild-type BlaC, BlaC G132S, and BlaC D179N (chapters 2 and 3).<sup>81,172</sup> Averaged chemical shift perturbations (CSPs) compared with wild-type BlaC were calculated and visualized on the crystal structure (Figure 4.4). The backbone amides of Phe105 and Ser106 could not be assigned with certainty in the spectra of BlaC variants containing the mutation I105F, so the minimal chemical shifts with reference to unassigned peaks were determined and used to calculate the CSPs. The CSPs for BlaC I105F are local and only present in the alpha helix containing the mutation side and the SDG motif (Figure 4.4 and S4.4). Due to the proximity of residues 105 and 132, with only 2.9 Å between the carbonyl group of 105 and the backbone amide of 132, the regions with chemical shifts overlap. Areas that are affected by both mutations show additive CSPs (Figure 4.5). For other areas, like the Ω-loop, only the effect of G132S is visible. The  $\text{C}_\alpha$ -atoms of Ile105 and Asp179 are 17.6 Å apart, and the CSPs of the two mutations only overlap for Ala135 and

Asn136 in the loop behind the SDG motif. All other residues in BlaC I105F+D179N either feel the effect of I105F or D179N. BlaC G132S+D179N clearly shows additive effects on CSPs for residues that are affected in both single mutants (Figure 4.5). The CSPs observed for the triple mutant are similar to those of BlaC G132S+D179N (Figures 4.4 and S4.4).

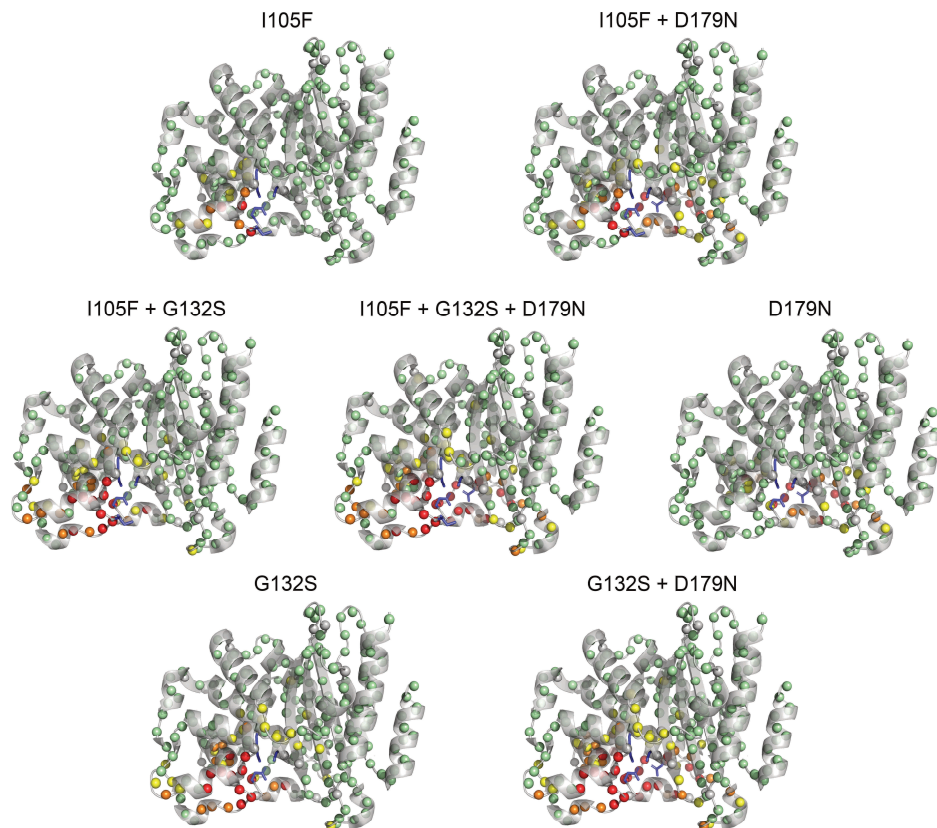


**Figure 4.4.** Average CSPs for the single, double, and triple mutants of BlaC plotted on the crystal structure of wild-type BlaC (PDB entry 5NJ2<sup>81</sup>). The backbone amides are represented as spheres and CSPs of greater than 0.025, 0.05, and 0.1 ppm are colored yellow, orange, and red, respectively; those with no or small CSPs are colored green, and the ones for which no data are available are in gray. The catalytic residues Ser70, Lys73, and Glu166 are represented as sticks, as are the mutated residues.

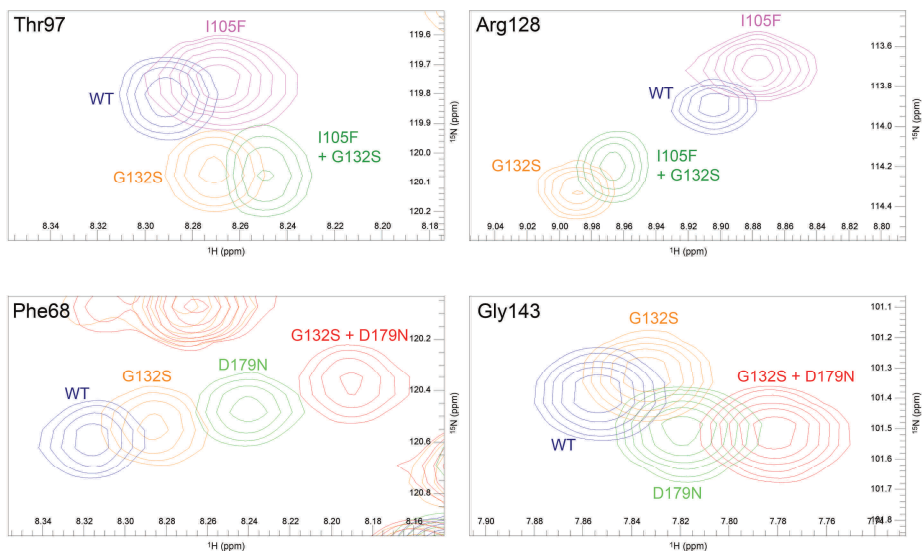


**Figure 4.5.** Overlay of  $^1\text{H}$ ,  $^{15}\text{N}$ -TROSY HSQC spectra of BlaC wild type (blue), I105F (pink), G132S (orange), D179N (bright green), I105F+G132S (dark green), G132S+D179N (red) showing additive effects on the chemical shifts.

**Table 4.2.** Overview of epistatic effects for the BlaC variants. Effects on ampicillin, sulbactam, and avibactam sensitivity as observed for cells expressing the BlaC variants, as well as the effect on thermostability and chemical shift perturbation of the backbone amides: +, positive epistasis; -, negative epistasis; 0, additive effect; ND, not determined.

BlaC variant	Ampicillin	Sulbactam	Avibactam	$T_m$	CSPs
I105F+G132S	0	+	-	0	0
I105F+D179N	+	0	ND	0	0
G132S+D179N	0	+	-	0	0
I105F+G132S+D179N	0	+	-	0	0

## Discussion

Three previously characterized mutations that each have a different effect on the wild-type BlaC were combined to study potential epistatic effects. All three double mutants show hints of positive epistasis, although in different ways (Table 4.2). BlaC I105F+G132S and G132S+D179N are less sensitive to sulbactam than the sum of their individual mutations *in vivo*, while BlaC I105F+D179N shows this effect for ampicillin. These effects could be caused by an increase in the level of active protein in the cell for both BlaC I105F and D179N, which would be in line with the observed increase in thermostability of both the I105F and D179N mutations. Higher enzyme levels make the cells less sensitive to substrates and inhibitors because the turnover capacity for both is higher. Similarly, it can explain the reduced sensitivity for avibactam in BlaC D179N. This agrees with the findings that screening for an increase in both stability and activity during multiple rounds of laboratory evolution eventually results in more activity than only screening for activity.<sup>17</sup> In this respect, it may appear surprising that the sensitivity of BlaC G132S to avibactam cannot be compensated to some degree by enhanced stability or substrate hydrolysis provided by the mutations I105F and D179N *in vivo*. For wild-type BlaC, the rate of avibactam hydrolysis is very low,<sup>102</sup> while hydrolysis of sulbactam is relatively fast.<sup>95</sup> Thus, the former acts as a stable, reversible inhibitor whereas the latter is a slowly converted substrate. For a substrate, a steady state exists of substrate that diffuses toward the cells and substrate that is hydrolyzed. Increased levels of active enzymes will be able to handle a higher substrate concentration. For a reversible inhibitor, an equilibrium, rather than a steady state, is reached between free and inhibited enzymes. A higher enzyme concentration does not affect the equilibrium, as long as the inhibitor concentration is much larger still.

The question remains why BlaC G132S is more sensitive to avibactam. As the avibactam hydrolysis rate is already low, it seems unlikely that a further reduction in the hydrolysis rate would cause this phenotype. It could be that either the affinity or acylation rate for avibactam is higher or that the adduct is tightly bound to the active site for BlaC G132S, resulting in a low deacylation rate. Avibactam would occupy the active site for a longer amount of time, blocking the enzyme from hydrolyzing the substrate. Most class A  $\beta$ -lactamases have an Asn in position 132, and mutating this to Gly results in increased resistance to avibactam for Bla<sub>Mab</sub>, CTX-M-15, and KPC-2.<sup>117,145</sup> The loop covering the active site in BlaC G132S is structurally more similar to this loop in CTX-M-15 and KPC-2 than wild-type BlaC, but BlaC G132S lacks the amide group that forms a hydrogen bond with the carbonyl of avibactam (Figure 4.6a).<sup>187,188</sup> The changes in the loop result in a blockage of the entrance to the active site that lowers the affinity of BlaC G132S for sulbactam, and the sulbactam adduct is stabilized by a hydrogen bond with the S104. Compared to sulbactam, the avibactam adduct is positioned further away from this loop, as the sulfate moiety of avibactam occupies the oxyanion hole between Ser70 and Thr237 (Figure 4.6b). These structural changes are likely the basis for the changes in avibactam sensitivity, yet the exact mechanism remains elusive. Interestingly, laboratory evolution experiments using BlaC G132S as a template to screen for avibactam

resistance did not yield any new mutations and resulted in the reversal of BlaC G132S to the wild-type enzyme (data not shown). This hints at resistance to sulbactam not being compatible with resistance against avibactam, making them interesting candidates for combination therapy using multiple inhibitors. In conclusion, it was found that combining two of the three mutations I105F, G132S, and D179N in BlaC results in both additive and epistatic effects.

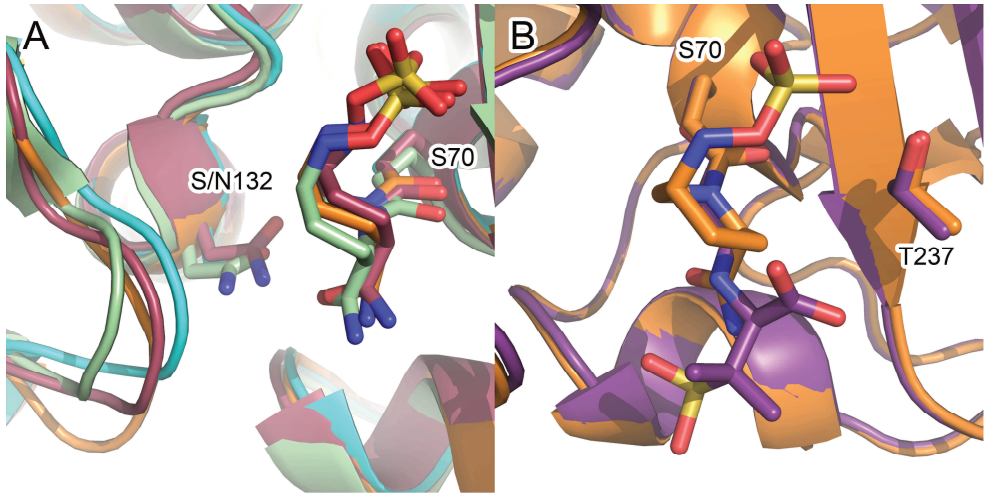


**Figure 4.6.** Structural differences between BlaC and other class A  $\beta$ -lactamases. (A) The loop covering the active site in BlaC G132S (PDB entry 7A71<sup>172</sup>, cyan) is more similar to CTX-M-15 (PDB entry 4HBU<sup>188</sup>, maroon) and KPC-2 (PDB entry 4ZBE<sup>187</sup>, green), both with the avibactam-adduct, than wild-type BlaC with the avibactam adduct (PDB entry 6H2H<sup>104</sup>, orange). (B) Overlay of BlaC structures with the avibactam (as in panel A) and sulbactam adducts (PDB entry 6H2K<sup>104</sup>, purple).

## Materials and methods

### Antibiotic and inhibitor susceptibility

Susceptibility was tested in *E. coli* KA797 expressing pUK21-*blaC* variants with a Tat-signal sequence (Figure S2.12).<sup>172</sup> Droplets of 10  $\mu$ L of liquid culture with optical densities 0.3, 0.03, 0.003, and 0.0003 were applied to LB agar plates with various concentrations of ampicillin, sulbactam, or avibactam. All plates contained 50  $\mu$ g mL<sup>-1</sup> kanamycin and 1 mM IPTG and were incubated for 16 hours at 37 °C and imaged using Gel Doc XR+ (Bio-Rad) and ImageLab 6.0.1 (Bio-Rad). To visualize changes in resistance, cell growth was scored with a value between -1 (more sensitive than wild type) and 4 (more resistant).

### Protein production

<sup>15</sup>N-labeled protein was produced using *E. coli* BL21 (DE3) pLysS cells transformed with pET28a plasmids containing the *blaC* gene with an N-terminal His-tag and TEV cleavage site (Figure 2.S2).<sup>172</sup> Protein was produced and purified as described before.<sup>81</sup>

### Thermal shift assay

Melting temperatures of the purified BlaC variants were determined using the hydrophobic dye SYPRO Orange Protein Gel Stain (diluted to 4x from a 5000x stock as supplied by Sigma-Aldrich) and using a CFX96 Touch Real-Time PCR detection system (Bio-Rad). Protein samples were diluted to a final concentration of 15  $\mu$ M in 100 mM sodium phosphate (pH 6.4). The temperature (T) was increased from 20 to 90 °C in steps of 1 °C, and samples were incubated for 1 min at each temperature before detection of the fluorescence signal. Measurements were performed in triplicate. Data were analyzed using OriginPro version 9.1 (OriginLab) and fit using equation 4.1:

$$y(T) = A_2 + \frac{A_1 - A_2}{1 + e^{(T-T_m)/dT}} \quad (4.1)$$

where A1 and A2 are the initial and final values of fluorescence, respectively, T<sub>m</sub> is the melting temperature in degrees Celsius, and dT describes the steepness of the change in fluorescence upon unfolding.

### NMR experiments

TROSY-HSQC<sup>150,151</sup> spectra for all mutants were obtained at 25 °C using a Bruker AVIII HD 850 MHz spectrometer equipped with a TCI cryoprobe. Samples contained ca. 0.3 mM <sup>15</sup>N BlaC or <sup>13</sup>C,<sup>15</sup>N BlaC in 100 mM sodium phosphate (pH 6.4) and 6 % D<sub>2</sub>O. Data were processed with Topspin 4.0.6 (Bruker Biospin) and analyzed using CCPNmr Analysis V2.<sup>152</sup> Spectra were assigned by comparing them to the TROSY-HSQC and HNCA spectra of wild-type BlaC<sup>81</sup>, BlaC

G132S (chapter 2)<sup>172</sup>, and BlaC D179N (chapter 3) and average chemical shift perturbations (CSPs) of backbone amides were calculated using equation 4.2:

$$\Delta\delta = \sqrt{\frac{1}{2}\left(\Delta\omega_1^2 + \left(\frac{\Delta\omega_2}{5}\right)^2\right)} \quad (4.2)$$

where  $\Delta\omega_1$  and  $\Delta\omega_2$  are the differences in chemical shifts in spectra of the mutant and wild-type enzymes for  $^1\text{H}$  and  $^{15}\text{N}$ , respectively. For BlaC variants containing the mutation I105F, residues Phe105 and Ser106 could not be assigned to peaks, so the minimal chemical shift with reference to unassigned peaks was determined and used to calculate the CSP.

## Supporting information



**Figure S4.1** *In vivo* activity of BlaC variants in *E. coli*. Cells producing the different BlaC variants were spotted on plates containing indicated concentrations of ampicillin. “All 3” refers to I105F+G132S+D179N. BlaC S70A is catalytically inactive and functions as negative control.





**Figure S4.2** *In vivo* activity of BlaC variants in *E. coli*. Cells producing the different BlaC variants were spotted on plates containing  $10 \mu\text{g mL}^{-1}$  ampicillin and indicated concentrations of sulbactam. “All 3” refers to I105F+G132S+D179N. BlaC S70A is catalytically inactive and functions as negative control.



**Figure S4.3** *In vivo* activity of BlaC variants in *E. coli*. Cells producing the different BlaC variants were spotted on plates containing  $10 \mu\text{g mL}^{-1}$  ampicillin and indicated concentrations of avibactam. “All 3” refers to I105F+G132S+D179N. BlaC S70A is catalytically inactive and functions as negative control. The plate without avibactam is the same as the plate without sulbactam in Figure S4.2.

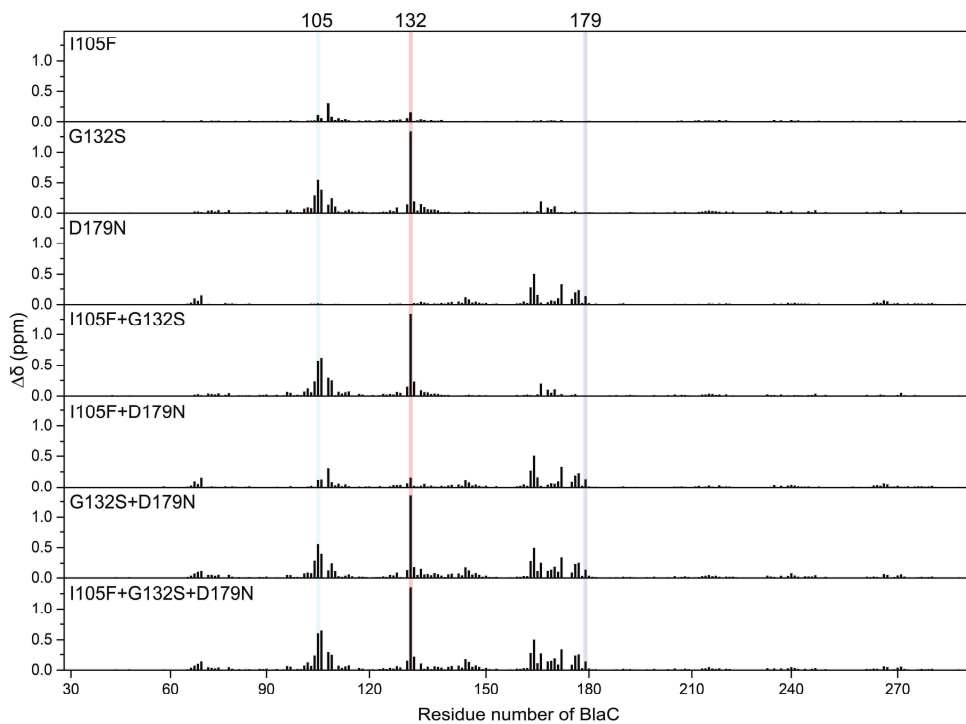


**Figure S4.4.** Average CSP for the backbone amides of the BlaC variants. Residue numbers refer to Ambler numbering (Figure 1.1).<sup>65</sup> The mutation sites are shaded blue, red, and purple, for residues 105, 132, and 179, respectively.